

Recent warming evidence inferred from a tree-ring-based winter-half year minimum temperature reconstruction in northwestern Yichang, South Central China, and its relation to the large-scale circulation anomalies

Qiufang Cai¹ · Yu Liu^{1,2} · Yanchao Wang³ · Yongyong Ma^{1,4} · Han Liu^{1,4}

Received: 23 September 2015 / Revised: 10 April 2016 / Accepted: 17 April 2016 / Published online: 2 May 2016
© ISB 2016

Abstract High-resolution winter temperature reconstructions in China are rare, yet vital for the comprehensive understanding of past climate change. In the present work, the first winter-half year minimum mean temperature from previous November to current April in northwestern Yichang, South Central China, was reconstructed back to 1875 based on tree-ring material. The reconstruction can explain 55 % of the variance over the calibration period during 1955–2011. The temperature maintained at comparatively low level before 1958, and an abnormal warming was seen since 1959. However, the warming trend stagnated after 2000 AD. 2001–2010 was the warmest decade not only during the instrumental period but also during the whole reconstructed period. The reconstruction indicates good spatial resemblance to other temperatures series in adjacent areas and Northern Hemisphere, yet the recent warming in this study is earlier and more prominent than that of Southeast China. This work also manifests that the winter-half year minimum temperature in study area has good agreement with summer (June–September) maximum temperature variation in Southeast

China at decadal scale, except that the winter-half year warming in recent decades is more evident than summer. This reconstruction is not only useful in improving our knowledge of long-term temperature variation but also useful in predicting the tree growth dynamics in the future in the study area.

Keywords Tree-ring width · *Pinus massoniana* Lamb. · South Central China · Winter-half year minimum temperature · East Asian winter monsoon · Sea surface temperatures

Introduction

Temperature is not only one of the most crucial factors for vegetation distribution and food production but also a prerequisite to the stable development of human society (Liu et al. 2009a; Zhang et al. 2010; Büntgen et al. 2011). The global warming trend, significant especially during recent 30 years was reported by IPCC (IPCC 2013). Anxieties about the vulnerability of ecological environment and agricultural productions are increasing. Recent studies have shown that there was obvious seasonal asymmetry of temperatures variation (Gou et al. 2008; Cohen et al. 2012; Xia et al. 2014), indicating as more obvious winter temperature increase than in summer (Liu and Chen 2000; IPCC 2007; Liu et al. 2009b; Huang et al. 2012), which will possibly in turn regulate almost all biogeochemical processes (Schwartz et al. 2006; Piao et al. 2007). Therefore, evaluation of the status of modern warming should consider this non-uniform rate of climate warming between seasons (Xia et al. 2014), and more reconstructions focused on different seasons are needed.

Long-term temperature reconstructions based on different geological and biological proxies are very precious to extend our understanding of past climate variability beyond instrumental period and to evaluate the status of current climate

✉ Qiufang Cai
caiql@ieecas.cn

✉ Yu Liu
liuyu@loess.llqg.ac.cn

¹ The State Key Laboratory of Loess and Quaternary Geology, Institute of Earth Environment, Chinese Academy of Sciences, Xi'an 710075, China

² Department of Environmental Science and Technology, School of Human Settlements and Civil Engineering, Xi'an Jiaotong University, Xi'an 710049, China

³ Department of Geography, Xingtai University, Xingtai 054001, China

⁴ University of Chinese Academy of Sciences, Beijing, China

within the historical framework (Ljungqvist 2010; Zhang et al. 2010). Well-dated tree rings are such good natural archives and have been widely used in regional to hemispheric climatic reconstructions for the last hundreds to thousands of years because of their accurate dating, high resolution, and widespread coverage (Yadav et al. 1999; Büntgen et al. 2011; Pederson et al. 2014; Yang et al. 2014).

Tree-ring-based temperature reconstructions have been widely reported in Northern and Southwest China, however, few in Southern China. In the existing researches mainly focused on spring-summer (Liang et al. 2008; Cai et al. 2010, 2013; Chen et al. 2013; Duan and Zhang 2014; Li et al. 2015) and annual temperature reconstructions (Fan et al. 2008; Li et al. 2014), the winter-time (hereafter refers to different month combinations from previous September to current May) temperature variations are rarely reported (Zhu et al. 2009; Gou et al. 2008; Liu et al. 2009a, 2009b). It is believed that winter-half year temperature (October–April) was closely related with the grain yield during the last two millennia in China (Yin et al. 2014). Even though the existing studies highlighted the temperature variations in China, the characteristics of winter-time temperature have not been well recognized so far. There is still a strong need for high-resolution paleo-data on winter-time temperature to strengthen spatial coverage and comprehensive understanding of past climate and to reduce the uncertainty of climate change awareness in history (Zheng et al. 2010).

Tree rings in Southeast China have great potential in reflecting winter-time temperature variation (Shi et al. 2010; Chen et al. 2012; Duan et al. 2012). How about the tree rings in South Central China? The objectives of this study were (1) to develop a new tree-ring chronology in Hubei Province, South Central China, (2) to investigate tree growth-climate relationship and reconstruct the winter-half year minimum temperature variation from previous November to current April since 1875, and (3) to detect the possible triggers of temperature variation in the study area. Results of this study are helpful to answer the following two questions: (1) Is recent warming in the study area evident? (2) Does seasonal asymmetry of temperature variation in Southern China exist?

Materials and methods

Study area and tree-ring materials

The study area belongs to the Dabashan Mountain extension. It is located in the mountainous area of northwestern Yichang Municipality, Hubei Province, in the south central region of China (Fig. 1). It has a humid subtropical monsoon climate. The annual mean temperature generally ranges from 16.5 to 22 °C, recorded from the two nearest meteorological stations (Fig. 1). January (4.3 °C) and July (28.0 °C) are the coldest

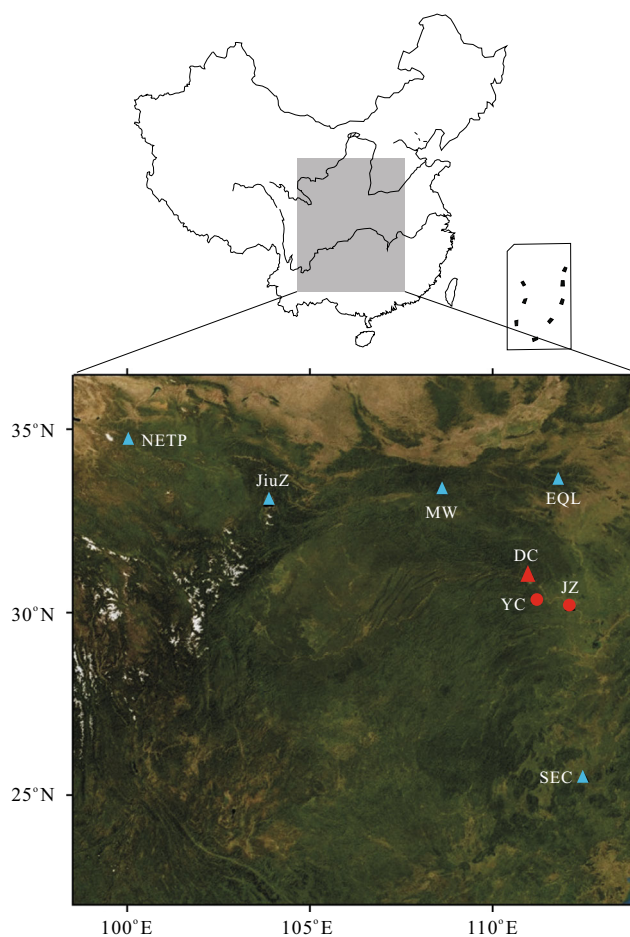


Fig. 1 Map showing the locations of the sampling site (red triangle), the meteorological stations (red dots), and the compared sites (blue triangles). JZ Jingzhou, YC Yichang, SEC Southeast China (Duan et al. 2012), EQL eastern Qinling Mountains (Shi et al. 2009), MW Muwang (Liu et al. 2009b) in the southern slope of Qinling Mountains, JiuZ Jiuzhaigou region (Song et al. 2007), NETP northeastern Tibetan Plateau (Gou et al. 2008)

and hottest months, respectively. The annual mean total precipitation is about 1280 mm, with 70.3 % mainly occurs from May through October. The mean annual evaporation is around 950 mm, with relatively high humidity (82 %). The soil type in the sampling site (named DC, 31.02° N, 111.00° E, 900–940 m a.s.l.) is yellow soil, which is rich in organic matter. Masson pine (*Pinus massoniana* Lamb.) is the dominant tree species, generally growing up to more than 20 m high. It is accompanied by young trees including *Lindera megaphylla* Hemsl., *Cinnamomum bodinieri* Levl., and *Ficus virens* Ait. var. *sublanceolata* (Miq.) Corner. and dense shrubs including *Lespedeza bicolor* Turcz. and *Vitex negundo* L. The trees grow in a small hill with flat top, and the tree canopies are comparatively open. Using increment borer, 55 cores from 33 healthy Masson pine trees with one or two cores from each tree were collected.

The tree-ring cores were processed according to standard dendrochronological techniques (Stokes and Smiley 1996).

All cores were mounted to the special wooden frames after air dried, and then they were polished with different mesh sand paper until the tree-ring boundaries were clear. In case of missing ring or false ring occurred, cross dating was done by applying the traditional skeleton plot method to assign calendar year to each growth ring. Then the tree rings in each core were measured to the nearest 0.001 mm using the LINTAB measuring device, which was connected with a binocular microscope and TSAP software (Rinn 1996). The results of cross dating and ring-width measurements were evaluated by the COFECHA program (Holmes 1983).

Standardization is a basic step in dendrochronology to remove the non-climate trend related to tree age or the effects of stand dynamics in order to better isolate climate-related growth variations (Fritts 1976). Conservative detrending method (CDM) generally uses negative exponential curve or straight line with negative slope as fitted curves to each raw measurement series and index for each core is calculated by dividing the actual ring width by the corresponding fitted value. Then all the single indexes are combined together to produce a standard tree-ring chronology. It is generally implemented in the ARSTAN program (Cook and Kairiukstis 1990). However, this conservative method is thought to be imperfect in preserving long-timescale climatic variance (Briffa et al. 1992, 1996). In order to overcome this limitation, Briffa et al. (1992) introduced the “Regional Curve Standardization” (RCS) method to dendroclimatology by applying one-regional-curve as fitted curve to all individual measurement serials, and this RCS method was adopted in many studies (Esper et al. 2002; Büntgen et al. 2008). Recently, a “Signal Free” (SF) method during standardization approach was introduced (Melvin and Briffa 2008; Briffa and Melvin 2011), which is thought to be useful to reduce or remove the distortion in the expressed external forcing signal. In the present work, the SF method combined with the CDM and RCS methods were employed to produce the SF-CDM and SF-RCS chronologies through the CRUST software (see Melvin and Briffa 2014 for more details), respectively. The reliable starting years of the chronologies were estimated using the subsample signal strength (SSS) threshold (Wigley et al. 1984) because few samples existed at the early years. Usually, the tree-ring chronology is qualified when SSS > 0.85. To further evaluate the quality of the chronology, inter-series correlation coefficient (R_{bar}) and the expressed population signal (EPS) were calculated over 50 years lagged by 25 years (Wigley et al. 1984).

Climate data

There are two meteorological stations near the sampling site: Jingzhou (JZ, 30.2° N, 112.11° E, 32.6 m a.s.l., 1954–2011) and Yichang (YC, 30.42° N, 111.18° E, 134.3 m a.s.l., 1952–2011). Monthly climatic records including the maximum

mean temperature (T_{max}), minimum mean temperature (T_{min}), mean temperature (T_{mean}), and monthly total precipitation (P) were collected. Climatic records from these two stations indicated almost uniform variations both on monthly and annual scale (Fig. 2). The mean annual total precipitation amounts in these two stations showed comparatively stable variation without obvious trends (Fig. 2c), while the annual mean temperatures showed an increasing tendency ($p < 0.01$) (Fig. 2d). The climate data in the two stations were highly correlated. The correlation coefficient (r) between the mean minimum temperature records from previous November to current April from the two stations was 0.90 ($p < 0.001$) (Fig. 2e), indicating good agreement of regional climate. Therefore, the data from the two meteorological stations were arithmetically averaged to represent the regional climate information during 1954–2011.

Statistical analysis

Pearson’s correlation analysis between the tree-ring chronologies and meteorological records during their common period was conducted to detect the climate-growth relationship and to determine which climatic factor is the limiting factor and suitable for final reconstruction. Monthly climatic data within a time-window from previous October to current September and seasonal combinations were analyzed against the tree-ring chronologies. Based on the knowledge of above tree growth-climate relationship analysis, a linear regression model was therefore developed to reconstruct the target climatic factor. To test the fidelity of our reconstruction in imitating the actual data, the data sets were divided into two parts (1955–1982 and 1983–2011) for the calibration and verification cross check. The statistical parameters included the Pearson’s correlation coefficient (r), R -squared (R^2), sign test (ST), product means (t), reduction of error (RE), and coefficient of efficiency (CE) (Fritts 1976; Cook et al. 1999). To estimate the expected range of variability of 11-year running mean that may arise stochastically, we employed the Monte Carlo approach (Neumaier and Schneider 2001; Schneider and Neumaier 2001) to generate 10,000 synthetic temperature time series, each of the same length as the reconstructed temperature time series. For each synthetic time series we calculated 11-year running mean and the 2.5th and 97.5th percentiles of the 11-year average values from all 10,000 synthetic time series were defined as the 95 % confidence interval. To reveal the temporal and spatial representativeness of the reconstruction, spatial correlation analyses between the SF-RCS chronology, the reconstructed temperature, and the CRU TS3.22 gridded dataset were conducted according to KNMI Climate Explore (<http://climexp.knmi.nl>). Moreover, the reconstructed temperature was compared not only with several existing tree-ring-based winter-time temperature

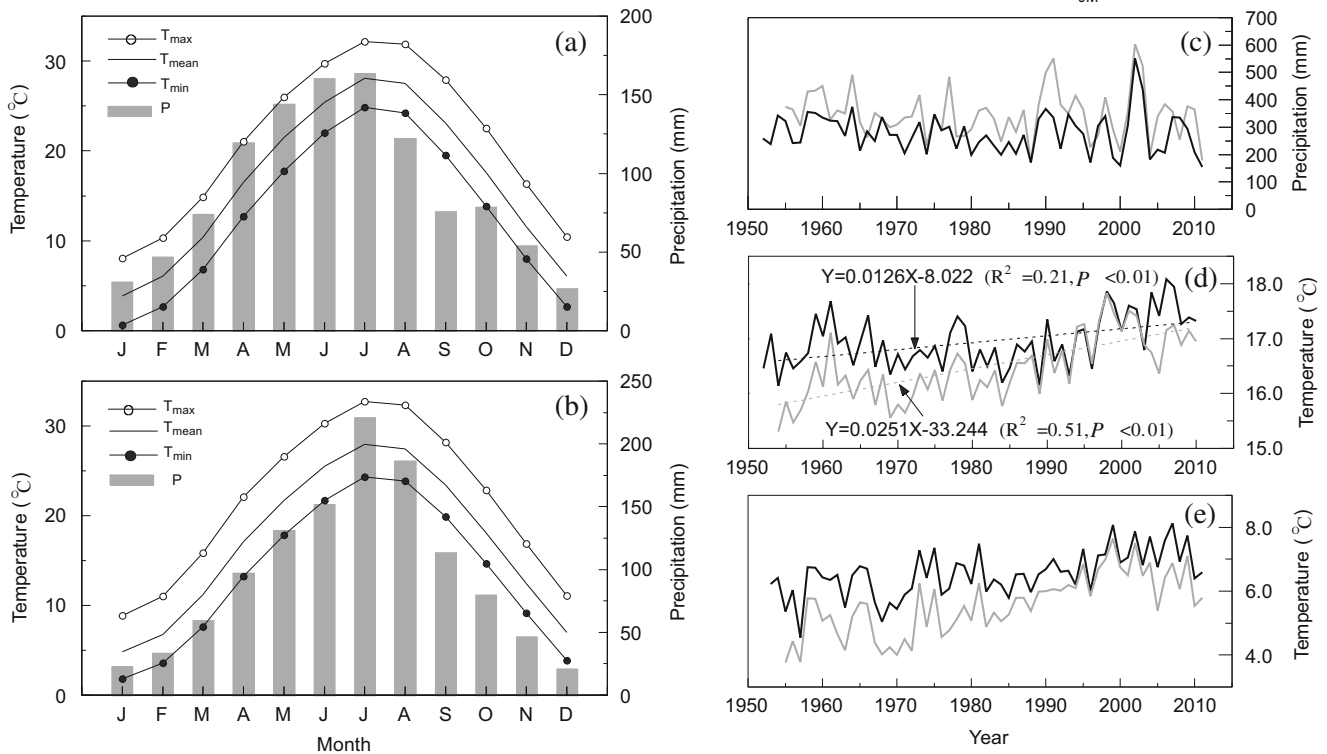


Fig. 2 Monthly climate variations in JZ (a) and YC (b) stations and annual total precipitation (c), annual mean temperature (d), and annual mean minimum temperature variations from previous November to

current April (e) of the two stations during their instrumental periods. Dashed lines in (d) indicate the linear trends of temperatures

reconstructions in China (Song et al. 2007; Gou et al. 2008; Liu et al. 2009b; Shi et al. 2009; Duan et al. 2012) but also with the previous November–current April Northern Hemispheric (NH) temperature variations (<http://www.cru.uea.ac.uk/cru/data/tem2/tavenh2v.dat>). To investigate if there exists seasonal temperature asymmetry in Southern China, the reconstructed temperature was compared with the summer (June–September) maximum temperature variations in Macheng, Southeast China (Cai and Liu 2013).

Results

Tree-ring chronologies

The SF-CDM and SF-RCS chronologies spanning from 1857 to 2011 were finally developed based on 46 cores from 29 trees, respectively. The reliable starting year of the chronology was 1875; 15 cores from 12 trees existed at that year (Fig. 3). The mean EPS value during the common period 1900–2010 was 0.91, higher than the acceptable threshold 0.85 (Wigley et al. 1984), and Rbar values were comparatively stable during the whole period. The two chronologies showed accordant variation ($r = 0.983, p < 0.001$).

Tree growth–climate relationship

As shown in Fig. 4, both the SF-CDM and SF-RCS chronologies indicated similarly positive correlations with monthly temperatures from previous November through current July, particularly significant with the monthly mean and minimum mean temperatures (Fig. 4a, c), while no significant relationship was found between the chronologies and monthly

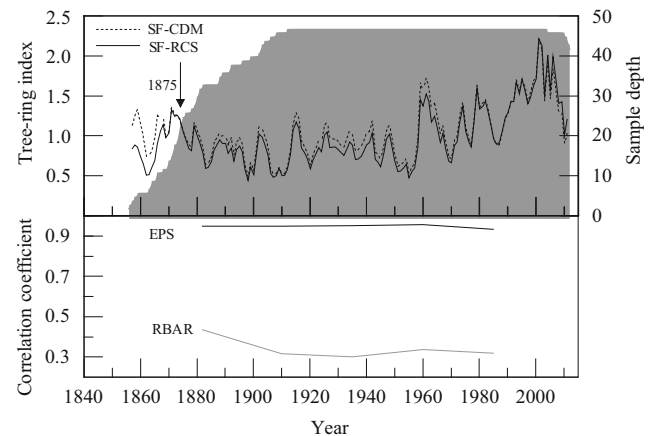


Fig. 3 Different methods developed tree-ring chronologies from the Masson pines. The arrow indicates the starting year indicated by SSS >0.85

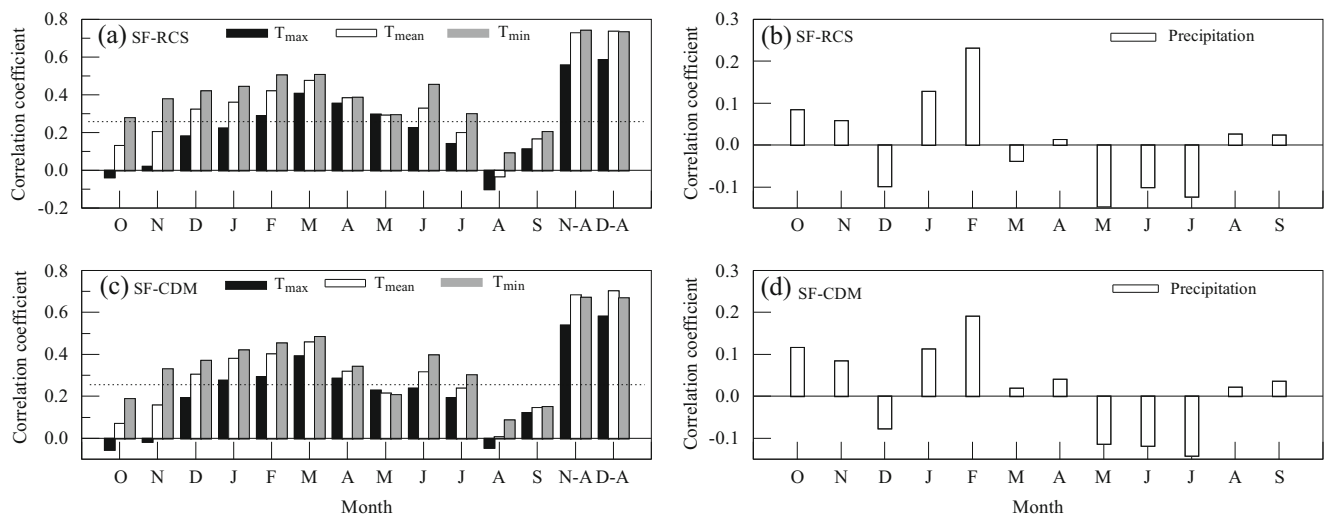


Fig. 4 Correlation analyses between SF-RCS (a, b), SF-CDM chronologies (c, d), and regional maximum (black bars), mean (white bars), minimum (grey bars) temperatures and precipitations. Dotted lines indicate the 95 % confidence level

precipitation (Fig. 4b, d). Moreover, the SF-RCS chronology was a little bit superior to the SF-CDM chronology in response to climate. The highest correlation was found between the SF-RCS chronology and the different combination of winter-time temperatures. The correlation coefficient (r) with the mean minimum temperature from previous November to current April (T_{\min_N-A}) was 0.741 ($p < 0.001$) and 0.738 ($p < 0.001$) with the mean temperature from previous December to current April ($T_{\text{mean_D-A}}$). Our results are consistent with previous tree-ring studies of *P. massoniana* in neighborhood of Southeastern China (Duan et al. 2012) and Taiwan Pine from the Yangtze River (Shi et al. 2010), demonstrating that winter-time temperature is the most important factor that influences the radial growth of trees in South Central through Southeastern China.

Spatial correlation analysis between the SF-RCS chronology and the CRU TS3.22 gridded data disclosed that the tree-ring chronology had significant correlations not only with the T_{\min_N-A} in the studied area but also with the concurrent temperature of a wide range of China (Fig. 5a), which was very similar to that of the observed temperature (Fig. 5b). We should also point out that after detrending the tree-ring chronology and CRU gridded temperatures, the spatial correlation patterns still existed at least in Southeastern China, although the significance reduced (Fig. 5c). Thus, the following temperature reconstruction in the study area will be regionally representative to a great extent.

The winter-half year minimum temperature reconstruction and variability

According to the above analysis, the winter-half year minimum mean temperature from previous November to current April (T_{\min_N-A}) was reconstructed based on a simple linear

regression model using the SF-RCS chronology as the predictor.

$$T_{\min_N-A} = 4.048 + 1.588 \times \text{SF-RCS}_t$$

$$(r = 0.741, n = 57, R^2 = 55\%, R^2_{\text{adj}} = 54.2\%, F = 67.149)$$

Here, t refers to the current year. This regression model extended the instrumental T_{\min_N-A} back to 1875. The reconstruction accounted for 55 % (54.2 % after adjustment for the loss of degrees of freedom) of the instrumental temperature over the calibration period from 1955 to 2011. The reconstructed temperature exhibited well agreement to the observation (Fig. 6a) and considerable fluctuations on both the annual and decadal scales (Fig. 6b).

The results of split calibration-verification test are shown in Table 1. Both Pearson's correlation coefficients (r) and the product means test (t) values for all the calibration and verification periods were significant at the 0.01 level. ST results were significant at the 99 % confident level during calibration periods and significant at the 95 % confident level during verification periods. Both parameters, i.e., RE and CE were positive, indicating sufficient skill existed in the reconstruction in predicting the observation (Cook et al. 1999).

Given the reconstruction can explain 55 % variance in the instrumental temperature, and the correlation coefficient (r) between the two first difference series of reconstructed and instrumental temperature was 0.48 ($p < 0.01$), the low-frequency variation of the reconstruction is more reliable than high-frequency. Therefore, the reconstruction was 11-year moving averaged to highlight the decadal-scale variation (Fig. 6b). The results of the Monte Carlo approach indicated the confidence interval of the reconstruction lay between 4.7038 and 6.5885 °C. The decadal variance of the reconstructed temperature before the late 1980s may arise stochastically (Fig. 6b). A pronounced warming since 1959 was seen

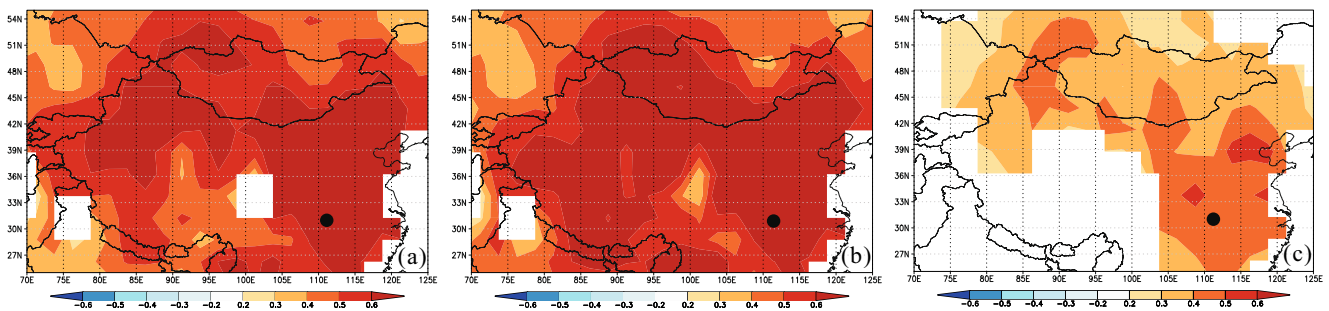


Fig. 5 Spatial correlation fields between the SF-RCS chronology (a), instrumental $T_{\min N-A}$ in the study area (b) and CRU TS3.22 gridded data during 1955–2011. Spatial correlation pattern between the detrended series of the tree-ring chronology and CRU gridded temperatures (c).

in the reconstruction, which indicated that our reconstruction had the ability to capture global warming signal. However, the warming trend stagnated after 2000 AD. 2001–2010 was recorded as the warmest decade (mean value = 6.74 °C) not only during the instrumental period from 1955 to 2011 (mean value was 6.07 °C) but also during the whole reconstructed period since 1875 (mean value was 5.62 °C) (Fig. 6b). The reconstructed temperature remains low before 1958. Even though,

The plots are created through KNMI Climate Explorer (<http://climexp.knmi.nl>). The black dot shows the general location of the sampling site (a–c)

the temperature values during 1875–1895 and 1925–1948 were comparatively higher than the temperature value during 1898–1912. The reconstructed temperature indicated considerably synchronous variations with the winter-time temperatures in different regions of Southern China (Fig. 8).

Discussions

Why tree-ring growth is limited by winter-half year temperature?

Different from dendroclimatological investigations in Northern China, where tree growth was mainly limited by current growth season climatic factors (Liang et al. 2008, 2010; Fang et al. 2012; Cai et al. 2014), most recent studies in Southern China suggested that radial growth of coniferous trees were mainly limited by previous winter-time temperature (Liu et al. 2009b; Shi et al. 2010; Duan et al. 2012). This is also true in our study site, where tree growth positively correlated with winter-half year mean (minimum) temperature at significant level. The study site belongs to a humid area with annual precipitation above 1000 mm, precipitation amount from May to October accounts for about 70.3 % of annual mean. Good combination of sufficient water and heat during the growth season is beneficial for tree growth. Thus, neither precipitation nor temperature in the growth season limits the radial growth of the tree. In previous winter, although the cambium activity has stopped, high temperature can protect the tree root from low-temperature frostbite on the one hand, and on the other hand, the warm winter is favorable for producing non-structural carbohydrates and other organic material, which were stored in tree and might be used for tree growth in the following growth season (Shi et al. 2009). On the contrary, low winter temperature may increase freezing injury to tree roots and then destroy and limit the normal activity of tree (Duan et al. 2012). Furthermore, high temperature in spring can stimulate the meristematic activities in the following growth season to start in advance; therefore, the growth season will be prolonged and wide ring will appear, and the contrary when the spring

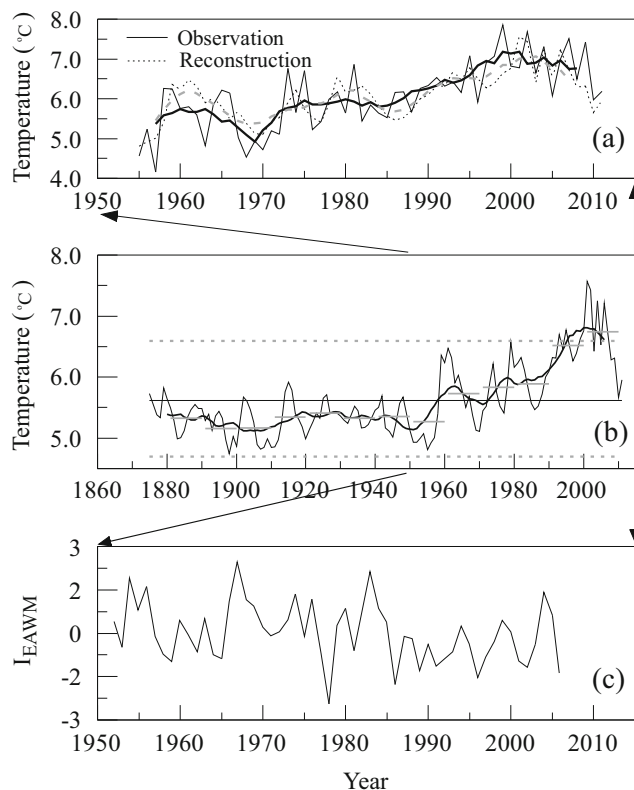


Fig. 6 (a) Comparison between the reconstructed and observed $T_{\min N-A}$. Bold lines are 5-year moving average. (b) Temperature reconstruction from 1875 to 2011. The bold black line is the 11-year moving average, the long horizontal line represents the average value of 1875–2011, horizontal bold grey lines indicate values of every 10-year average, and the dashed lines indicate the 95 % confidence interval. (c) East Asian winter monsoon (EAWM) index (Zhu 2008)

Table 1 Calibration and verification statistics for the tree-ring reconstruction of winter-half year temperature

	Calibration (1955–1983)	Verification (1984–2011)	Calibration (1983–2011)	Verification (1955–1982)	Full calibration (1955–2011)
r	0.589**	0.682**	0.683**	0.586**	0.741**
R^2	34.7 %	46.6 %	46.7 %	34.3 %	55 %
CE	–	0.124	–	0.143	–
RE	–	0.683	–	0.613	–
t	5.394**	5.517**	6.075**	6.472**	6.643**
ST	24+/5**	20/8–*	23/6–**	19+/8*	40+/17–**

r Pearson's correlation coefficient, R^2 R-squared, ST sign test, t product means, RE reduction of error, CE coefficient of efficiency (Fritts 1976; Cook et al. 1999)

*Significance at the 95 % confidence level

**Significance at the 99 % confidence level

temperature is low. From what has been discussed above, the limitation of previous winter-half year temperature on the tree growth of following year has specific physiological significances. If the previous winter-half year temperature keeps rising in the future, it will greatly favor the *P. massoniana* tree growth in the study area.

The limiting effect of previous winter-time temperature was widely reported for different species in humid Southern China, such as *Pinus taiwanensis* Hayata and *P. massoniana* in Southeast China (Shi et al. 2010; Chen et al. 2012; Duan et al. 2012) and *Abies fargesii* in Shennongjia (Dang et al. 2013; Zheng et al. 2016). The significant positive relationship between winter-time temperature and tree growth was also reported in eastern Qinling Mountains for *Pinus tabulaeformis* (Liu et al. 2009b), *Pinus armandii* Franch (Shi et al. 2009), and *Abies chensiensis* (Chen et al. 2015), and in Northeastern China for *Pinus koraiensis* (Zhu et al. 2009).

Spatial coherence of the winter-time temperature variations

Further spatial correlation fields showed that the reconstructed T_{\min_N-A} not only had significant correlation with concurrent temperature in most part of China but also global-scale correlation (Fig. 7a, b), indicating covariability of temperature in the study area and global temperature.

Comparisons between the reconstructed T_{\min_N-A} and other tree-ring-based winter-time temperature reconstructions in Southern China are provided to further reveal the spatial resemblance of winter-time temperature variation (Fig. 8). The T_{\min_N-A} in our study site (Fig. 8a) showed more synchronously warm-cold variations as that in the Southeastern China (SEC) (Duan et al. 2012; Fig. 8b) and the eastern Qinling Mountains (EQL) (Shi et al. 2009, Fig. 8c). All these three series indicated comparatively low temperatures around 1946–1955 and high temperatures during 1939–1944 and 1978–1985. During 1925–1934, our study area and EQL exhibited warm condition, while low temperature was seen in SEC (Fig. 8). Though all these series

indicated warming trends during recent decades, the warming phenomenon in our study site started since the 1950s, earlier than the other two regions, and the magnitude of warming was more prominent. It seems that the recent warming over the study area appeared intense with respect to global warming compared with its neighboring areas. In addition, the winter (November–February) maximum temperature reconstruction in Fujian, Southeast China, also witnessed the evident warming since the early 1950s (Chen et al. 2012).

Moreover, the unusual winter-half year warming during recent decades in our study is supported by tree-ring-based temperature reconstructions (Fig. 8d–f) from Muwang (MW), southern slope of Qinling Mountains (Liu et al. 2009b), Jiuzhaigou region (JiuZ) (Song et al. 2007), and northeastern Tibetan Plateau (NETP) (Gou et al. 2008), though their temperature variations during the earlier periods were not well matched. It is worth mentioning that roughly all the winter-time temperatures before 1970 in MW, JiuZ, and NETP (Fig. 8d–f) remained cool compared with recent warming, which are very similar to our study. Except for the above evidence from tree rings, our temperature reconstruction is also supported by the historical evidence (Hao et al. 2012b). Using the information regarding snowfall days from historical documents of the Yu-Xue-Fen-Cun archive, Hao et al. (2012b) reconstructed the winter (December–February) mean temperature for the middle and lower reaches of the Yangtze River (our study area was included). It indicated that the later half of the nineteenth century was extremely cold, and temperature in the early half of the twentieth century was also low compared with the later half of the twentieth century (please refer to Fig. 2 in Hao et al., 2012b). It convincingly corroborated that cold winter in the early part of our reconstruction did exist in South Central China.

The reconstructed T_{\min_N-A} also had good agreements with the Northern Hemispheric (NH) winter-half year temperature variations (<http://www.cru.uea.ac.uk/cru/data/tem2/tavenh2v.dat>) with $r = 0.542$ ($N = 125$, $p < 0.001$) (Fig. 8g) and further proved that our temperature reconstruction not only contained

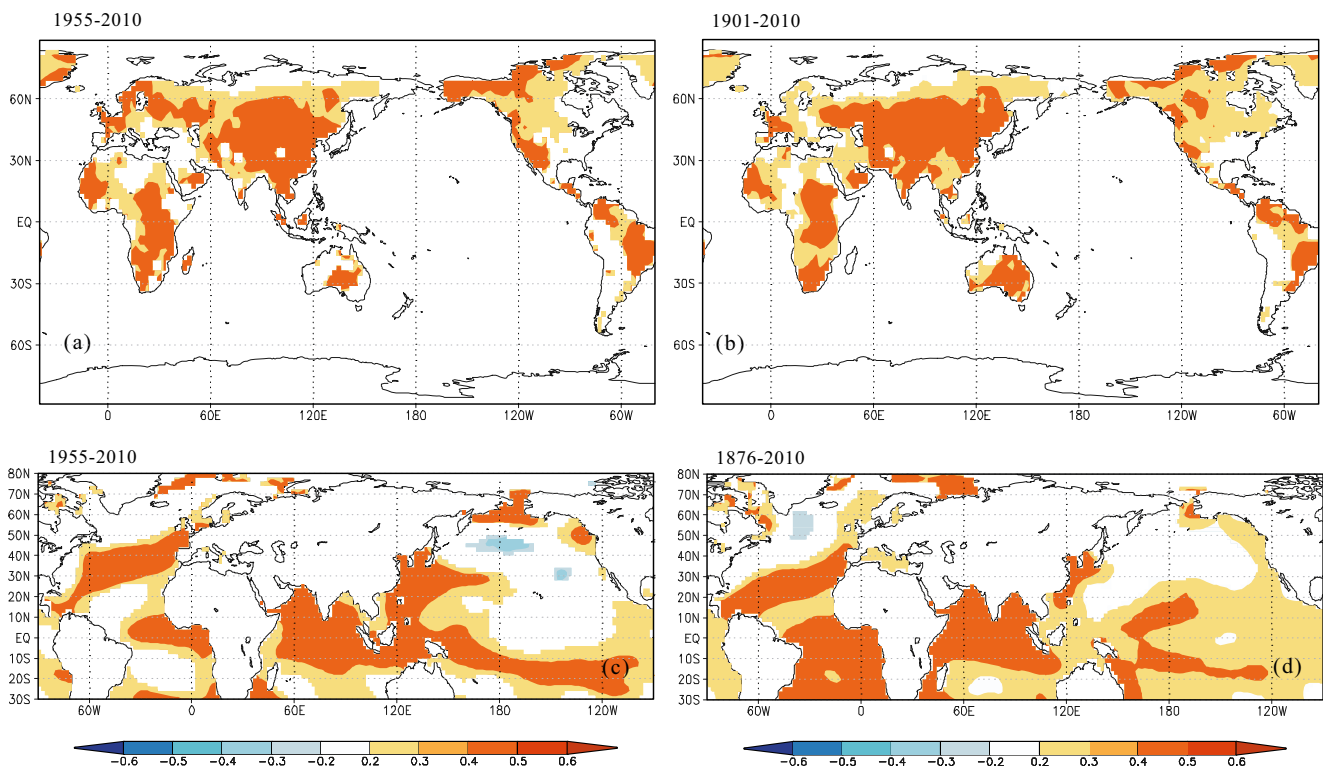


Fig. 7 Spatial correlation fields between the reconstructed temperature and global land gridded temperature (**a**, **b**) and global SST (**c**, **d**) at different time spans

local climate signal but also well-matched hemispheric temperature variation, as shown by the spatial field analysis (Fig. 7a, b).

Does winter temperature increases more evident than summer?

Although there are massive temperature reconstructions around the world, analysis of the seasonal difference of temperature variation is not extensively reported. Among the existing researches, some believed that the recent warming trend could be attributed to the temperature changes during winter (Liu and Chen 2000), while others thought that winter temperature did not show clearer warming than the other three seasons (Cohen et al. 2012).

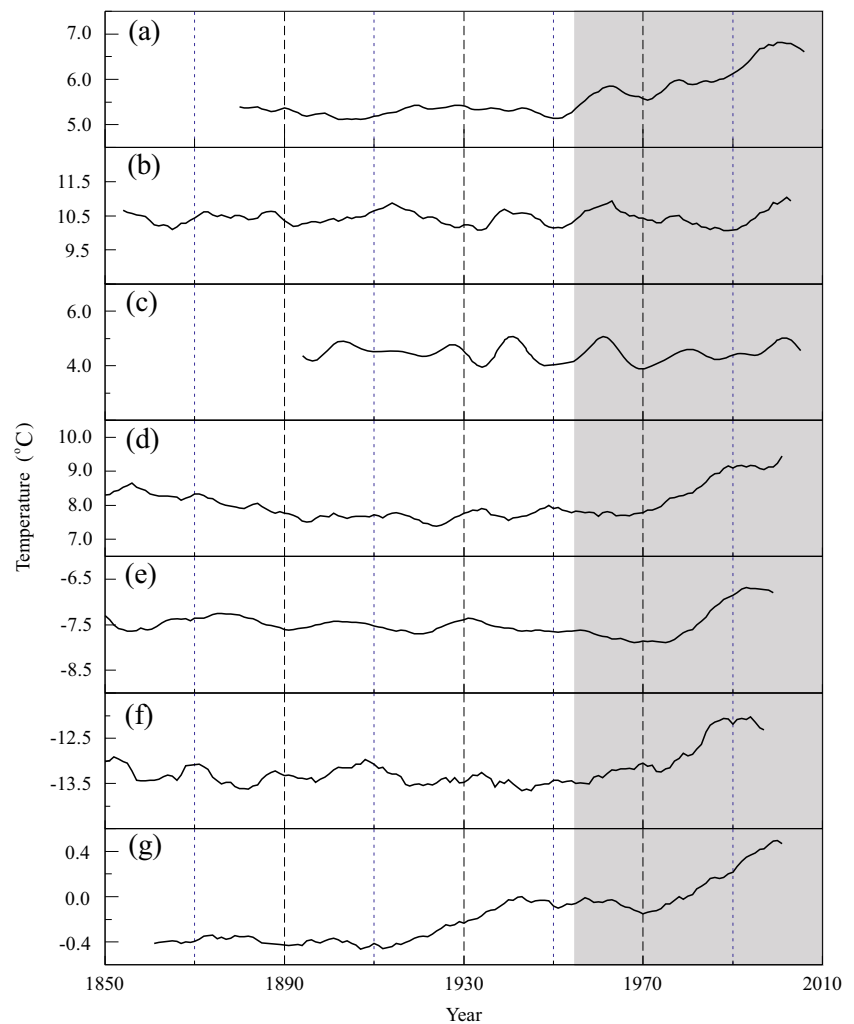
In our present work, the reconstructed winter-half year minimum temperature showed good agreement with the summer maximum temperature variations in Macheng, Southeast China (Cai and Liu 2013) (Fig. 9a) at decadal scale. However, discrepancy emerged since the 1970s when the winter-half year temperature in this study increased rapidly while the summer temperature in Macheng decreased till the end of 1980s and then increased. Obviously, the increasing amplitude of winter-half year temperature was much larger than that of summer. Moreover, the instrumental records of the study area also disclosed an evident increasing trend of winter-half year minimum temperature, while a decreasing trend was seen in

Macheng summer temperature before 1980, followed by a slowly increasing trend (Fig. 9b). Tree-ring evidence in the nearby Qinling Mountain range, Central China, also demonstrated more pronounced abnormal warming in winter (previous September–current April) than in summer (May–July) during recent decades (Liu et al. 2009b). Dendroclimatological study in northeastern Tibetan Plateau indicated an asymmetric variation patterns between the winter-half year (previous October–current April) minimum temperature and summer-half year (April–September) maximum temperatures, and the winter-half year minimum temperature increased more evident than the summer-half year maximum temperature (Gou et al. 2008). All the above cases likely manifest that winter-time warming may be the main contributor of recent warming in Southern China, but more evidences are needed to fully support such conclusion.

Superficial analysis of the possible mechanism of winter-half year minimum temperature variation

Mechanisms that cause the winter temperature variations in South Central China remain under study. Many studies showed that winter temperature variation in China was strongly impacted by the East Asian winter monsoon (EAWM), an important component of the climate system in East Asia, originating from the Siberian high, characterizing by a sudden establishment, a rapid southward movement, and strong winds

Fig. 8 Comparisons between this reconstruction (a) and other tree-ring-based winter temperature reconstructions in China (b–f) and instrumental winter-half year mean temperature of the NH (<http://www.cru.uea.ac.uk/cru/data/tem2/tavenh2v.dat>) (g). The January–April mean temperature in SEC (Duan et al. 2012) (b), the mean temperature from prior December to current April in EQL (Shi et al. 2009) (c), the mean temperature from prior September to current April in MW (Liu et al. 2009b) (d), the minimum mean temperature from prior November to current March in JiuZ (Song et al. 2007) (e), the minimum mean temperature from previous October to current April in NETP (Gou et al. 2008) (f). All the series are the 11-year moving average

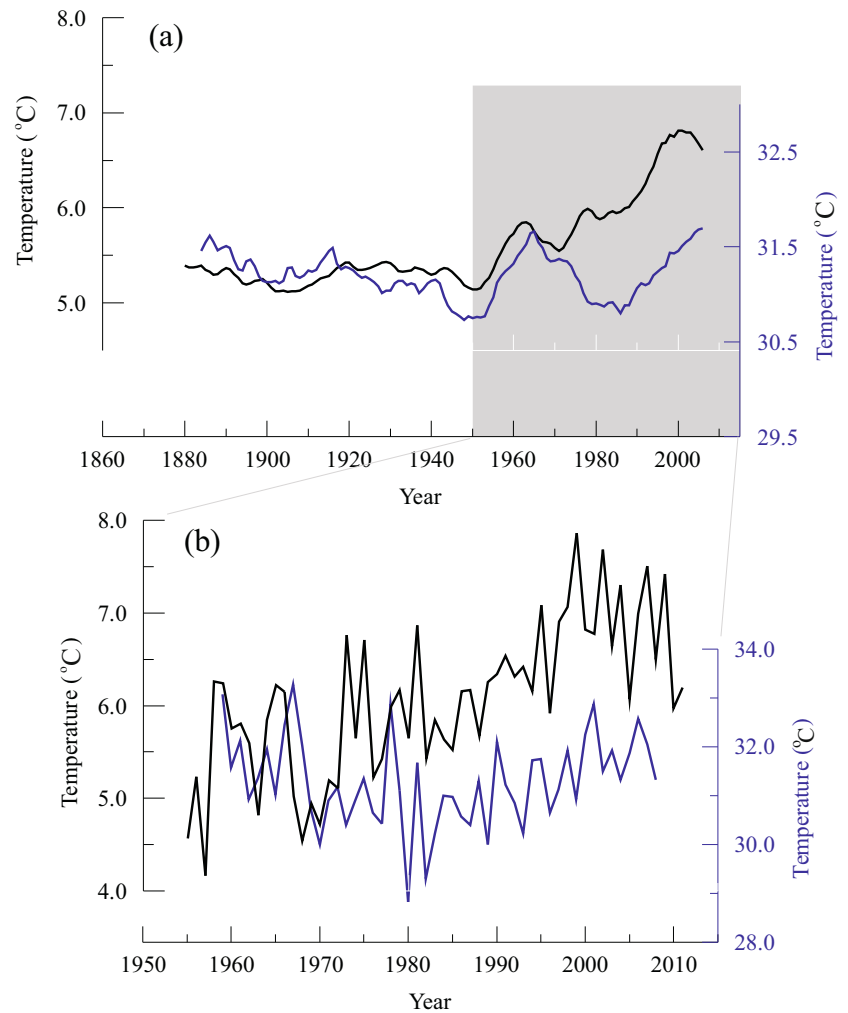


(Ding et al. 2014). When the EAWM is strong, winter temperature in China was comparatively low, and the contrary when the EAWM is weak (Zhu et al. 2009; Duan et al. 2012). In Fig. 6, the increasing trends of both the observed and reconstructed $T_{\min, N-A}$ were roughly opposite to the decreasing trend of EAWM index (Zhu 2008). It is worth noting that the decreasing trend of EAWM since mid-1980s was not obvious, while the increasing trend of winter-half year minimum temperature in our study area was still apparent. As we know, the EAWM index refers to the period from December of current year to February of next year (Zhu 2008), while our temperature reconstruction refers to the period from November of previous year to April of current year. The difference in seasons may be responsible for the discrepancy between them. Another possibility is that in addition to the EAWM influence, human activity or other undetected factors may also be responsible for the recent winter warming in South Central China. Similar conclusion was also drawn by Zheng et al. (2016) in the nearby Shenongjia region. Moreover, the running variance of the temperature reconstruction since the late 1980s exceeded the 95 % confidence interval for stochastic

variations (Fig. 6b), implying that the recent warming in the study area may be attributed to special external forcing, e.g., anthropogenic activity.

The anomalous distribution of ocean heat source is generally responsible for the large-scale circulation and the long-term climate anomalies. Previous studies proved that sea surface temperature (SST) anomalies in the Indo-Pacific region were closely associated with the strength of EAWM, by changing the land-sea thermal contrast, the fundamental driving force for the winter monsoon (Wang and He 2013). Chen et al. (2014) also pointed out that the winter temperature mode in China was closely related to the northeastern Siberian high (origin of EAWM) and SSTs over the Atlantic and Indian oceans. In this study, spatial correlation patterns also disclosed that the winter-half year minimum temperature variation was significantly and positively influenced by the concurrent SST in the tropical Indian Ocean (TIO), North Atlantic Ocean (NAO), and tropical western Pacific Ocean (TWPO) (Fig. 7c, d). By analyzing the 500 hPa geopotential height field and 850 hPa wind field, Hao et al. (2012a) suggested that the abnormal warming in winter-time SST in the TIO would

Fig. 9 (a) Comparison between the 11-year moving average of the reconstructed winter-half year minimum temperature (*black*) and summer maximum temperature in Macheng (*blue*). (b) Comparison between the instrumental winter-half year minimum temperature in the study area (*black*) and summer maximum temperature in Macheng (*blue*)



cause the weakening of EAWM. By applying the rotated varimax orthogonal rotation method and wavelet transformation, Qu et al. (2006) found that winter SST anomalies in central North Atlantic (CAN) had close relation with the winter temperature variation in China by motivating Eurasian circulation of EU pattern. When winter SST in CNA was abnormally high, the winter temperature in China (including our study area) was also high, and vice versa. Therefore, the abnormal SST variations in the TIO, NAO, and TWPO regions influence the winter-half year temperature variation in South Central China, possibly by influencing the strength of EAWM. About this theory, further researches are needed.

Conclusions

Using tree-ring cores collected from *P. massoniana* Lamb. in northwestern Yichang, South Central China, the minimum mean temperature from previous November to current

April during 1875–2011 was reconstructed. The new reconstruction exhibited cold winter before 1950s and abnormal warm winter since 1959. Comparisons indicated that the winter-half year temperature variation in the study area resembled the winter-time temperature variations in adjacent Southeast China and eastern Qinling Mountains and also have good agreement to the NH winter-half year temperature variation. However, the recent winter-half year warming in our study area was more pronounced than winter-time or summer warming in Southeast China. The abnormal recent winter warming and cold winter before 1959 is not only supported by the winter-time temperature reconstructions based on tree rings elsewhere but also historical documents in Southern China. EAWM could be the direct driving force of winter-half year temperature variation. Human activity may also play a role on the warming since the mid-1980s. In addition, abnormal SSTs in the TIO, TWPO, and NAO regions influenced the winter-half year minimum temperature variation in the study area by influencing the strength of EAWM.

Acknowledgments The authors would like to thank the Yiling District Forestry Bureau of Yichang City for the assistance in the field work. This work was jointly supported by the National Natural Science Foundation of China (41171170), CAS “Light of west China” program, the National Basic Research Program of China (2013CB955903), and the State Key Laboratory of Loess and Quaternary foundation (SKLLQG).

References

- Briffa KR, Jones PD, Bartholin TS, Eckstein D, Schweingruber FH, Karlén W, Zetterberg P, Eronen M (1992) Fennoscandian summers from AD 500: temperature changes on short and long timescales. *Clim Dyn* 7:111–119
- Briffa KR, Jones PD, Schweingruber FH, Karlén W, Shiyatov SG (1996) Tree-ring variables as proxy-climate indicators: problems with low frequency signals. In: Jones PD, Bradley RS, Jouzel J (eds) *Climatic variations and forcing mechanisms of the last 2000 years*. Springer, Berlin, pp. 9–41
- Briffa KR, Melvin TA (2011) A closer look at Regional Curve Standardization of tree-ring records: justification of the need, a warning of some pitfalls, and suggested improvements of its application. In: Hughes MK, Diaz HF, Swetnam TW (eds) *Dendroclimatology: progress and prospects*. Springer, pp. 113–145
- Büntgen U, Frank D, Grudd H, Esper J (2008) Long-term summer temperature variations in the Pyrenees. *Clim Dyn* 31:615–631
- Büntgen U, Tegel W, Nicolussi K, McCormick M, Frank D, Trouet V, Kaplan JO, Herzog F, Heussner KU, Wanner H, Luterbacher J, Esper J (2011) 2500 Years of European climate variability and human susceptibility. *Science* 331(6017):578–582
- Cai QF, Liu Y (2013) The June–September maximum mean temperature reconstruction from Masson pine (*Pinus massoniana* Lamb.) tree rings in Macheng, Southeast China since 1879 AD. *Chin Sci Bull* 58(Suppl.1):169–177 [in Chinese with English abstract]
- Cai QF, Liu Y, Bao G, Lei Y, Sun B (2010) Tree-ring-based May–July mean temperature history for Lüliang Mountains, China, since 1836. *Chin Sci Bull* 55(26):3008–3014
- Cai QF, Liu Y, Lei Y, Bao G, Sun B (2014) Reconstruction of the March–August PDSI since 1703 AD based on tree rings of Chinese pine (*Pinus tabulaeformis* Carr.) in the Lingkong Mountain, southeast Chinese loess Plateau. *Clim Past* 10:509–521
- Cai QF, Liu Y, Tian H (2013) A dendroclimatic reconstruction of May–June mean temperature variation in north China since 1767 AD. *Quat Int* 283:3–10
- Chen F, Yuan YJ, Wei WS, Yu SL, Zhang TW (2012) Tree ring-based winter temperature reconstruction for Changting, Fujian, subtropical region of Southeast China, since 1850: linkages to the Pacific Ocean. *Theor Appl Climatol* 109:141–151
- Chen F, Zhang RB, Wang HQ, Qin L (2015) Recent climate warming of Central China reflected by temperature-sensitive tree growth in the eastern Qinling Mountains and its linkage to the Pacific and Atlantic Oceans. *J Mt Sci* 12(2):396–403
- Chen Z, Wu RG, Chen W (2014) Distinguishing interannual variations of the northern and southern modes of the East Asian winter monsoon. *J Clim* 27:835–851
- Chen ZJ, Zhang XL, He XY, Davi NK, Cui MX, Peng JJ (2013) Extension of summer (June–August) temperature records for northern Inner Mongolia (1715–2008), China using tree rings. *Quat Int* 283:21–29
- Cohen JL, Furtado JC, Barlow M, Alexeev VA, Cherry JE (2012) Asymmetric seasonal temperature trends. *Geophys Res Lett* 39:L04705. doi:10.1029/2011GL050582
- Cook ER, Kairiukstis LA (1990) *Methods of dendrochronology: applications in the environmental sciences*. Kluwer Academic Publishers, Dordrecht, 394 pp
- Cook ER, Meko DM, Stahle DW, Cleaveland MK (1999) Drought reconstructions for the continental United States. *J Climatol* 12:1145–1162
- Dang HS, Zhang YJ, Zhang KR, Jiang MX, Zhang QF (2013) Climate-growth relationships of subalpine fir (*Abies fargesii*) across the altitudinal range in the Shennongjia Mountains, Central China. *Clim Chang* 117:903–917
- Ding YH, Liu YJ, Liang SJ, Ma XQ, Zhang YX, Si D, Liang P, Song YF, Zhang J (2014) Interdecadal variability of the East Asian winter monsoon and its possible links to global climate change. *J Meteor Res* 28(5):693–713
- Duan JP, Zhang QB (2014) A 449 year warm season temperature reconstruction in the southeastern Tibetan Plateau and its relation to solar activity. *J Geophys Res Atmos* 119:11578–11592
- Duan JP, Zhang QB, Lv LX, Zhang C (2012) Regional-scale winter-spring temperature variability and chilling damage dynamics over the past two centuries in Southeastern China. *Clim Dyn* 39:919–928
- Esper J, Cook ER, Schweingruber FH (2002) Low frequency signals in long tree-ring chronologies for reconstructing past temperature variability. *Science* 295:2250–2253
- Fan ZX, Bräuning A, Cao KF (2008) Annual temperature reconstruction in the central Hengduan Mountains, China, as deduced from tree rings. *Dendrochronologia* 26:97–107
- Fang KY, Gou XH, Chen FH, Liu CZ, Davi N, Li JB, Zhao ZQ, Li YJ (2012) Tree-ring based reconstruction of drought variability (1615–2009) in the Kongtong Mountain area, Northern China. *Glob. Planet Change* 80–81:190–197
- Fritts HC (1976) *Tree rings and climate*. Academic Press, London
- Gou XH, Chen FH, Yang MX, Jacoby G, Fang KY, Tian QH, Zhang Y (2008) Asymmetric variability between maximum and minimum temperatures in Northeastern Tibetan Plateau: evidence from tree rings. *Sci China Ser D Earth Sci* 51(1):41–55
- Hao LS, Ding YH, Kang WY, Xiang L (2012a) Relationship between the Indian Ocean SST change and summer precipitation reduction in North China. *Clim Chang Res Lett* 1:13–21 [in Chinese with English abstract]
- Hao ZX, Zheng JY, Ge QS, Wang WC (2012b) Winter temperature variations over the middle and lower reaches of the Yangtze River since 1736 AD. *Clim Past* 8:1023–1030
- Holmes RL (1983) Computer-assisted quality control in tree-ring dating and measurement. *Tree-Ring Bull* 43:69–75
- Huang J, Guan X, Ji F (2012) Enhanced cold-season warming in semi-arid regions. *Atmos Chem Phys* 12:5391–5398
- IPCC (2007) *IPCC Fourth Assessment Report (AR4)*. Cambridge University Press, Cambridge
- IPCC (2013) *Summary for policymakers. Climate Change 2013: The Physical Science Basis*. In: T. F. Stocker et al., Eds., Cambridge University Press, Cambridge: 1–29
- Li MY, Wang LL, Fan ZX, Shen CC (2015) Tree-ring density inferred late summer temperature variability over the past three centuries in the Gaoligong Mountains, southeastern Tibetan Plateau. *Palaeogeogr, Palaeoclimatol* 422:57–64
- Li ZS, Liu GH, Wu X, Wang XC (2014) Tree-ring-based temperature reconstruction for the Wolong Natural Reserve, western Sichuan Plateau of China. *Int J Climatol*. doi:10.1002/joc.4207
- Liang EY, Shao XM, Qin NS (2008) Tree-ring based summer temperature reconstruction for the source region of the Yangtze River on the Tibetan Plateau. *Glob Planet Change* 61:313–320
- Liang EY, Wang YF, Xu Y, Liu B, Shao XM (2010) Growth variation in *Abies georgei* var. *smithii* along altitudinal gradients in the Sygera Mountains, southeastern Tibetan Plateau. *Trees* 24:363–373
- Liu XD, Chen BD (2000) Climatic warming in the Tibetan Plateau during recent decades. *Int J Climatol* 20:1729–1742

- Liu Y, An ZS, Linderholm HW, Chen DL, Song HM, Cai QF, Sun JY, Tian H (2009a) Annual temperatures during the last 2485 years in the mid-eastern Tibetan Plateau inferred from tree rings. *Sci China Ser D Earth Sci* 52(3):348–359
- Liu Y, Hans LW, Song HM, Cai QF, Tian QH, Sun JY, Chen DL, Simelton E, Seftigen K, Tian H, Wang RY, Bao G, An ZS (2009b) Temperature variations recorded in *Pinus tabulaeformis* tree rings from the southern and northern slopes of the central Qinling Mountains, Central China. *Boreas* 38(2):285–291
- Ljungqvist FC (2010) A new reconstruction of temperature variability in the extra-tropical Northern Hemisphere during the last two millennia. *Geogr Ann* 92 A (3): 339–351
- Melvin TM, Briffa KR (2008) A signal-free approach to dendroclimatic standardisation. *Dendrochronologia* 26:71–86
- Melvin TM, Briffa KR (2014) CRUST: software for the implementation of Regional Chronology Standardisation: part 1. Signal-Free RCS. *Dendrochronologia* 32:7–20
- Neumaier A, Schneider T (2001) Estimation of parameters and eigenmodes of multivariate autoregressive models. *ACM Trans Math Softw* 27:27–57
- Pederson N, Hessel AE, Baatarbileg N, Anchukaitis KJ, Cosmo ND (2014) Pluvials, droughts, the Mongol Empire, and modern Mongolia. *PNAS* 111(12):4375–4379
- Piao S, Friedlingstein P, Ciais P, Viovy N, Dmarty J (2007) Growing season extension and its impact on terrestrial carbon cycle in the Northern Hemisphere over the past 2 decades. *Glob Biogeochem Cycles* 21:GB3018
- Qu JH, Jiang ZH, Tan GR, Sun L (2006) Relation between interannual, interdecadal variability of SST in North Atlantic in winter and air temperature in China. *Scientia Geographica Sinica* 26(5):557–563 [in Chinese with English abstract]
- Rinn F (1996) TSAP-Reference Manual. Trank Rinn, Heidelberg
- Schneider T, Neumaier A (2001) Algorithm 808: ARfit—a MATLAB package for the estimation of parameters and eigenmodes of multivariate autoregressive models. *ACM Trans Math Softw* 27:58–65
- Schwartz M, Ahas R, Aasa A (2006) Onset of spring starting earlier across the Northern Hemisphere. *Glob Change Biol* 12:343–351
- Shi JF, Cook ER, Lu HY, Li JB, Wright WE, Sheng FL (2010) Tree ring based winter temperature reconstruction for the lower reaches of the Yangtze River in Southeast China. *Clim Res* 41:169–175
- Shi JF, Lu HY, Wan JD, Li SF, Nie HS (2009) Winter-half year temperature reconstruction of the last century using *Pinus armandii* Franch tree-ring width chronology in the eastern Qinling Mountains. *Quat Sci* 29:831–836 [in Chinese with English abstract]
- Song HM, Liu Y, Ni WM, Cai QF, Sun JY, Ge WB, Xiao WY (2007) Winter mean lowest temperature derived from tree-ring width in Jiuzhaigou Region, China since 1750 A.D. *Quat Sci* 27(4):486–491 [in Chinese with English abstract]
- Stokes MA, Smiley TL (1996) An introduction to tree-ring dating. The University of Arizona Press, Arizona, Tucson
- Wang HJ, He SP (2013) The increase of snowfall in Northeast China after the mid 1980s. *Chin Sci Bull* 58:1350–1354
- Wigley TML, Briffa KR, Jones PD (1984) On the average value of correlated time series, with applications in dendroclimatology and hydrometeorology. *J Appl Meteorol Climatol* 23:201–213
- Xia JY, Chen JQ, Piao SL, Ciais P, Luo YQ, Wan SQ (2014) Terrestrial carbon cycle affected by non-uniform climate warming. *Nat Geosci* 7:173–180
- Yadav RM, Park WK, Bhattacharyya A (1999) Spring-temperature variations in western Himalaya, India, as reconstructed from tree-rings: AD 1390–1987. *The Holocene* 9(1):85–90
- Yang B, Qin C, Wang JL, He MH, Melvin TM, Osborn TJ, Briffa KR (2014) A 3500-year tree-ring record of annual precipitation on the northeastern Tibetan Plateau. *PNAS* 111(8):2903–2908
- Yin J, Su Y, Fang XQ (2014) Relationships between temperature change and grain harvest fluctuations in China from 210 BC to 1910 AD. *Quat Int*. doi:10.1016/j.quaint.2014.09.037
- Zhang ZB, Tian HD, Cazelles B, Kausrud KL, Brauning A, Guo F, Stenseth NC (2010) Periodic climate cooling enhanced natural disasters and wars in China during AD 10–1900. *Proc Biol Sci* 277(1701):3745–3753
- Zheng JY, Shao XM, Hao ZX, Ge QS (2010) An overview of research on climate change in China during the past 2000 years. *Geogr Res* 29(9):1561–1570 [in Chinese with English abstract]
- Zhu HF, Fang XQ, Shao XM, Yin ZY (2009) Tree ring-based February–April temperature reconstruction for Changbai Mountain in Northeast China and its implication for East Asian winter monsoon. *Clim Past* 5:661–666
- Zhu YF (2008) An index of East Asian winter monsoon applied to description the Chinese mainland winter temperature changes. *Acta Meteorologica Sinica* 66(5):781–788
- Zheng YH, Shao XM, Lu F, Li Y (2016) February–May temperature reconstruction based on tree-ring widths of *Abies fargesii* from the Shennongjia area in Central China. *Int J Biometeorol*. doi:10.1007/s00484-015-1111-x